

Growth of Nanoporous Silica Spherical Particles by the Stöber Method Combined with Supramolecular Templating Approach

Naoki Shimura and Makoto Ogawa*[,1]

Graduate School of Science and Engineering, Waseda University, Nishiwaseda 1-6-1, Shinjuku-ku, Tokyo 169-8050

[1]Department of Earth Sciences, Waseda University, Nishiwaseda 1-6-1, Shinjuku-ku, Tokyo 169-8050

Received October 21, 2004; E-mail: makoto@waseda.jp

Nanoporous silica spherical particles with narrow particle size distributions (standard deviation: 0.03–0.22) were synthesized by the Stöber method combined with supramolecular templating approach using tetraethoxysilane and cetyltrimethylammonium chloride. The reaction was conducted at 276 K to observe particle growth. Particles formed after the reaction for ca. 0.5 h, as shown by the fact that the solution became turbid. After the reaction for 0.5 h, particles with an average particle size of 440 nm in diameter were collected by filtration. The particles grew until the silica source was completely consumed. This took 50 h under the present reaction condition. The average particle size reached to ca. 1.8 μm at this stage. The calcined particles were porous with the surface areas of 380–1060 $m^2 g^{-1}$ and the pore diameter of 1.6–2.0 nm.

Mesoporous silicas prepared by supramolecular templating approach have been investigated as adsorbents, catalysts, and nano-reactors owing to their large surface area, pore size uniformity, and possible surface engineering.[1–4] The morphology of mesoporous silicas is an important issue for their practical applications,[5] so that the syntheses of mesoporous silicas in such morphology as coating films,[6,7] self-standing films,[8–11] monoliths,[12,13] fibers,[14,15] hollow spheres,[15–25] and dense spheres[26–50] have been reported.

Mesoporous silica spherical particles with controlled size and size distribution are attractive materials for such uses as optics and chromatography.[50] Accordingly, the preparation of mesoporous silica spherical particles has been reported so far[26–50] utilizing various synthetic approaches including those based on emulsion chemistry[47] and using morphology template.[48] The Stöber method, which was developed for the preparation of silica spherical particles with controlled particle size,[51,52] was also employed to prepare surfactant templated mesoporous silica spherical particles.[26–35] The preparation of the mesoporous silica particles with the particle size of 60–2300 nm have been reported so far.[26–35] However, because there are many factors, such as chemical composition and synthetic temperature, which affect the particle sizes, the relationships between the synthetic condition and the particle size are not fully understood. In addition, the particle size of the reported spherical particles[26–35] was ca. 2 nm.

So further study on the preparation of nanoporous silica spherical particles with different size and pore geometry is worth investigating. In the present study, we prepared surfactant–silica spherical particles at a low temperature (276 K) in order to follow their growth and to investigate the particle size and nanostructures of the products.

Experimental

Materials. Tetraethoxysilane (abbreviated as TEOS) and cetyltrimethylammonium chloride (abbreviated as CTAC) were obtained from Tokyo Kasei Kogyo Co., Ltd. and were used without further purification. Sodium hydroxide, methanol and 28% aqueous ammonia solution were obtained from Kanto Chemical Co., Ltd. and were used without further purification.

Sample Preparation. The reaction was conducted at 276 K because the hydrolysis of TEOS and the condensation were slow enough to follow the particle growth. CTAC (0.211 g), deionized water (17.7 g), methanol (100 mL) and 28% aqueous ammonia solution (7.2 g) were mixed and the solution was shaken for 15 sec at room temperature and was subsequently aged at 276 K overnight in a sealed vessel. To which solution was added TEOS (0.368 mL) and then the mixture was shaken for 3 sec. The mixture was subsequently aged at 276 K. In this paper, the reaction time means the aging time after the addition of TEOS. The molar ratio of TEOS:CTAC:deionized water:methanol:ammonia was 1:0.4:774:1501:72. After the aging, particles were separated by vacuum filtration using membrane filters (pore diameter: 220 nm; Fuji Photo Film Co., Ltd.). Because there was precipitate at the bottom of the vessels after the reaction for ca. 5 h, the precipitate was dispersed by ultrasonication prior to the vacuum filtration. The filtration was conducted quickly (1.5–2 min) enough to assume that the increase of the particle size during the filtration was in the range of experimental error. The particles were washed with methanol and were dried at 333 K for a day. The as-synthesized samples were named as ASP (X), where X denotes the reaction time. In order to remove surfactants, the as-synthesized particles were calcined in air at 823 K for 10 h at a heating rate of 150 $K h^{-1}$. The calcined samples were designated as CSP (X). In order to investigate the origin of nanopores, we prepared particles without using CTAC (reaction time was 50 h), and these were separated by centrifugation (25000 rpm) at 276 K. The particles after the washing with methanol and drying at 333 K were calcined in air at 823 K for 10 h at a heating rate of 150 $K h^{-1}$.

Characterization. Scanning electron micrographs (SEM) were obtained on a Hitachi S-2380N scanning electron microscope. Prior to the measurements, the samples were coated with

Published on the web June 6, 2005; DOI 10.1246/bcsj.78.1154

gold. Particle size distributions and average particle sizes were obtained by SEM observation for no less than 50 primary particles. Thermogravimetric-differential thermal analysis (TG–DTA) curves were recorded on a Rigaku TG-8120 instrument at a heating rate of 10 K min^{-1} and using α-alumina as the standard material. ASP (5 h) (50 mg) were dissolved in 2.0 M sodium hydroxide aqueous solution (10 mL), and the remaining chloride ion presence was checked by the $AgNO_3$ test. CHN analysis was performed on a Perkin Elmer 2400 II instrument. X-ray diffraction (XRD) was performed on a RAD IB diffractometer (Rigaku) using monochromatic Cu Kα radiation, operated at 40 kV and 20 mA. The nitrogen adsorption/desorption isotherms of the calcined particles were measured at 77 K on a Belsorp 28SA instrument (Bel Japan Inc.). Prior to the measurements, the samples were dried at 393 K under vacuum for 3 h.

Results and Discussion

The mixture became homogeneous after the mixing. No precipitates were collected by the filtration before the reaction for 0.5 h, indicating that particles did not form or formed particles were smaller than the pore diameter (220 nm) of the membrane filter. After the reaction for ca. 0.5 h, the solution became turbid. White precipitates were observed at the bottom of vessels after the reaction for ca. 5 h.

By the filtration, white solids were obtained when the reaction time was longer than 0.5 h. The filtrate obtained when the reaction time was shorter than 10 h became turbid after standing at room temperature within a day. Since some silica source and CTAC remained in the filtrate at these stages, it was thought that particles formed by the condensation of the remaining silica during the standing.

SEM images of ASP (0.5 h), ASP (0.67 h), ASP (1 h), ASP (5 h), ASP (20 h), and ASP (50 h) are shown in Fig. 1. The as-synthesized particles possessed spherical shapes irrespective of the reaction time. The particle grew to be ca. 1.7 μm in diameter after the reaction for 20 h. No further particle enlargement was observed by the prolonged reaction. The particle size distributions of ASP (0.5 h), ASP (0.67 h), ASP (1 h), ASP (5 h), and ASP (50 h) are shown in Figs. 2(a), (b), (d), (e), and (g), respectively, and the standard deviations and the coefficient of variations are summarized in Table 1. There is a general tendency toward broader particle size distribution as the reaction time increased. The SEM images of ASP (20 h) and ASP (50 h) shows the presence of 2–3 μm particles at this stage. These results are thought to be derived from the heterogeneity of the reactions. Since the reaction was conducted without stirring, a part of the formed particles precipitated; the amount of the precipitate increased as the reaction continued. As a result, heterogeneous nucleation and/or coagulation of the formed particles may occur to give a broader particle size distribution.

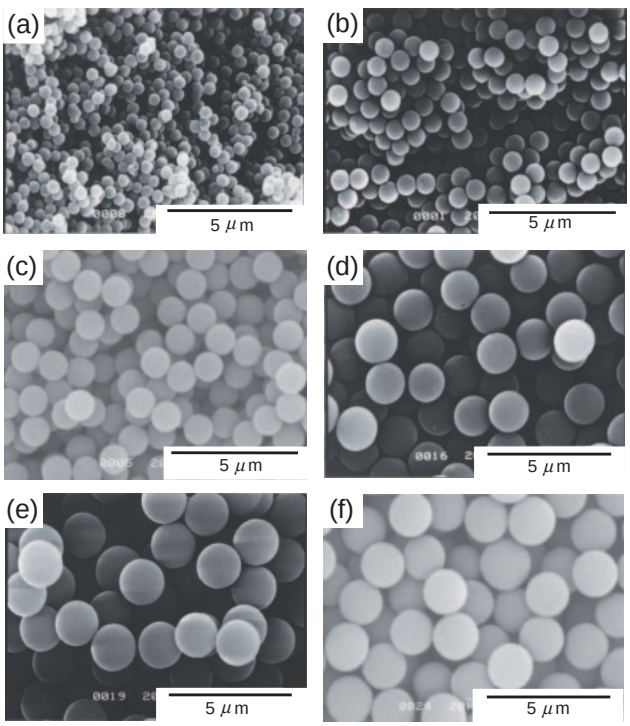

Fig. 1. SEM images of (a) ASP (0.5 h), (b) ASP (0.67 h), (c) ASP (1 h), (d) ASP (5 h), (e) ASP (20 h), and (f) ASP (50 h).

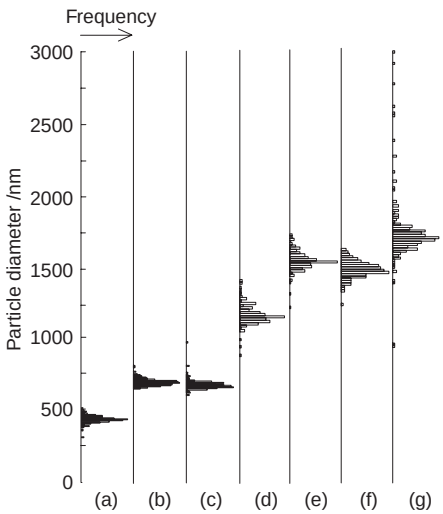

Fig. 2. Particle size distributions of (a) ASP (0.5 h), (b) APS (0.67 h), (c) CSP (0.67 h), (d) ASP (1 h), (e) ASP (5 h), (f) CSP (5 h), and (g) ASP (50 h).

Table 1. Average Particle Diameters, Standard Deviations and Coefficient of Variations (Abbreviated as CV) of ASP (0.5 h), ASP (0.67 h), ASP (1 h), ASP (5 h), and ASP (50 h)

Sample	Sample size	Average particle diameter/μm	Standard deviation/μm	CV/%
ASP (0.5 h)	230	0.44	0.026	6.0
ASP (0.67 h)	232	0.70	0.025	3.6
ASP (1 h)	211	1.17	0.072	6.2
ASP (5 h)	205	1.56	0.065	4.2
ASP (50 h)	227	1.75	0.218	12.4

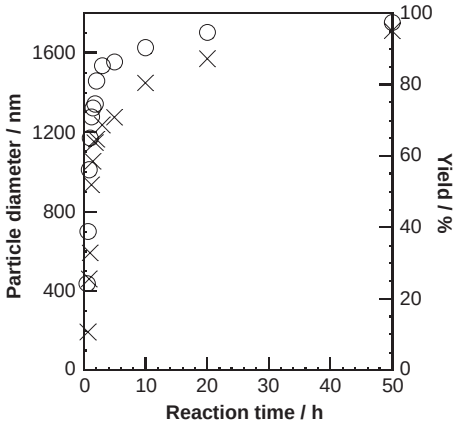

Fig. 3. Average particle sizes (○) and yields (silica base) (×) as a function of reaction time.

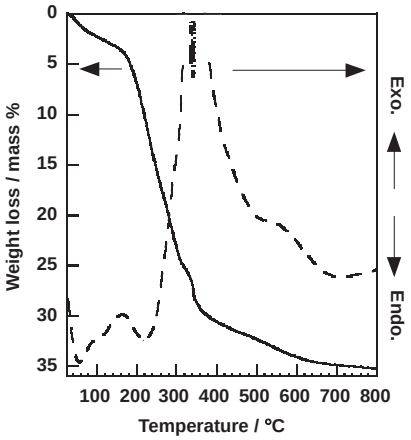

Fig. 4. TG–DTA curves of ASP (5 h).

Figure 3 shows the average particle sizes of the as-synthesized particles as a function of the reaction time. The particles rapidly grew at the initial stage of the reaction (−2 h) and the average particle size reached to ca. 1.5 μm when the reaction time was 2 h. Further gradual enlargement was observed and the average particle size became ca. 1.8 μm for ASP (20 h) and ASP (50 h).

In order to discuss the termination of the particle growth and nanostructures of the products, we determined product yields (silica base) considering the molar surfactant/Si ratios of the as-synthesized particles. TG–DTA curves of ASP (5 h) are shown in Fig. 4 as an example. The $AgNO_3$ test of ASP (5 h) was negative, indicating that the as-synthesized particles did not contain any chloride anions. Cetyltrimethylammonium cation (abbreviated as CTA^+)/Si ratios were derived from the TG curves as follows. The TG curves of the as-synthesized particles showed the weight losses at around 150–650 °C accompanying endothermic peaks in the corresponding DTA curves ascribable to the oxidative decomposition of CTA^+ and the condensation of the remaining silanol groups in the silica walls.[53,54] The weight losses at around 150–650 °C of ASP (5 h) shown in Fig. 4 were 31 mass%. The CTA^+ content of ASP (5 h) calculated from CHN analysis (C and N contents of 22.4 and 1.4 mass%, respectively) was 28.0 mass%. The molar C/N ratio of the ASP (5 h) determined by the CHN analysis was 19.2. This value is consistent with the molar C/N ratio of CTAC (C/N = 19.0), indicating that the presence of other organics such as ethoxy group from TEOS were negligible. Since most of the weight losses at around 150–650 °C was ascribable to the oxidative decomposition of CTA^+ (ca. 90%), the weight loss at 150–650 °C was assumed to be due to the oxidative decomposition of CTA^+. Therefore, the molar CTA^+/Si ratios of the as-synthesized particles were determined as shown in Fig. 5.

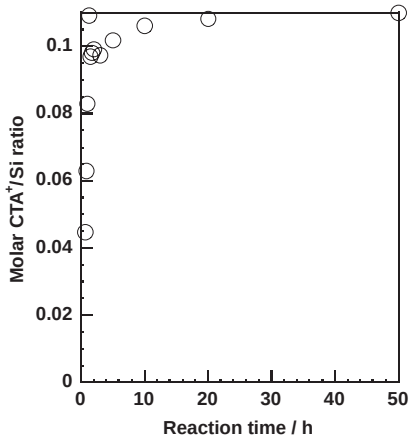

Fig. 5. The molar CTA^+/Si ratios of the as-synthesized particles.

The molar CTA^+/Si ratios of the as-synthesized particles increased with prolonging reaction time to 1.5 h, and reached a constant value of ca. 0.1 after the reactions for 10 h. This result showed that the particles grew with a heterogeneity of the chemical compositions.

The product yields (silica based) thus obtained are shown in Fig. 3. The yields rapidly increased at the initial stage of the reaction (−2 h). Further gradual increases of the yields were observed, and the yield reached to ca. 100% when the reaction time was 50 h. The average particle size increased with the increase of the yields until the yields attained to ca. 100% (the reaction time was 50 h). This result indicated that the particles grew until the silica source was completely consumed. Thus, it is suggested that the particle size could be controlled by the quantity of the silica source in the starting solutions.

The average particle size and the yields continued to increase until the silica source was completely consumed, as shown in Fig. 3. These results suggested that the particles, which formed when the reaction time was shorter than 0.5 h, grew and that the number of particles was unchanged. In other words, the number of particles that formed when the reaction time was shorter than 0.5 h determined the particle size.

SEM images of CSP (0.67 h) and CSP (5 h) are shown in Fig. 6. The particle morphology maintained after the calcination at 823 K for 10 h. Particle size distributions of CSP (0.67 h) and CSP (5 h) are shown in Figs. 2(c) and (f), respectively. The particle sizes decreased upon the surfactant removal, as a result of the condensation of the remaining silanol groups in the silica walls during the calcination. The decrease ratios of the average particle sizes by the calcination were only ca. 3% (from 0.70 μm to 0.68 μm) and ca. 4% (from 1.56 μm to 1.49 μm) for CSP (0.67 h) and CSP (5 h), respectively, so

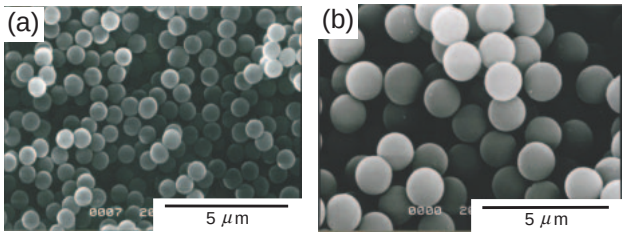

Fig. 6. SEM images of (a) CSP (0.67 h) and (b) CSP (5 h).

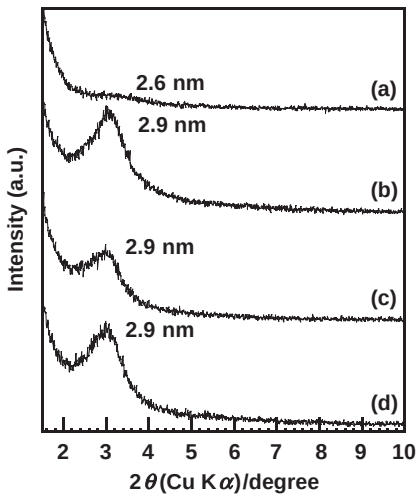

Fig. 7. XRD patterns of (a) CSP (0.67 h), (b) CSP (1 h), (c) CSP (2 h), and (d) CSP (50 h).

that the formation of porous particles could be assumed.

XRD patterns of CSP (0.67 h), CSP (1 h), CSP (2 h), and CSP (50 h) are shown in Fig. 7. Single peaks were observed at the lower 2θ regions ($d = 3$ nm) in the XRD patterns of all the calcined particles, indicating that the particles possessed ordered structures. The assignments of the diffraction patterns are not clear at present.

The nitrogen adsorption/desorption isotherms of CSP (0.67 h), CSP (1 h), CSP (2 h), and CSP (50 h) are shown in Fig. 8. The Brunauer–Emmett–Teller (BET) surface areas[55] of CSP (0.67 h), CSP (1 h), CSP (2 h), and CSP (50 h) were determined by the isotherms to be 380, 810, 980, and 1060 $m^2\,g^{-1}$, respectively. As the reaction time became longer, greater BET surface areas were observed. This was consistent with the results shown in Fig. 5, which shows the increasing CTA^+ contents with the particle growth.

The nitrogen adsorption isotherm of calcined particles prepared without using CTAC was followed type II, indicating that the particles were nonporous. This result suggested that the CTA^+ played a role as a supramolecular template.

The pore volumes were determined by the nitrogen adsorption isotherms (relative pressure was ca. 0.2). The pore volumes of CSP (0.67 h), CSP (1 h), CSP (2 h), and CSP (50 h) were 0.15, 0.33, 0.38, and 0.43 $mL\,g^{-1}$, respectively.

The pore size distributions (Fig. 9) of the calcined particles were derived from the nitrogen adsorption isotherms (Fig. 8) by the Barrett–Joyner–Halenda (BJH)[56] method. The pore size ranges from 1.6 for CSP (1 h) to 2.0 nm for CSP (50 h). This suggests that the heterogeneity of the chemical compositions

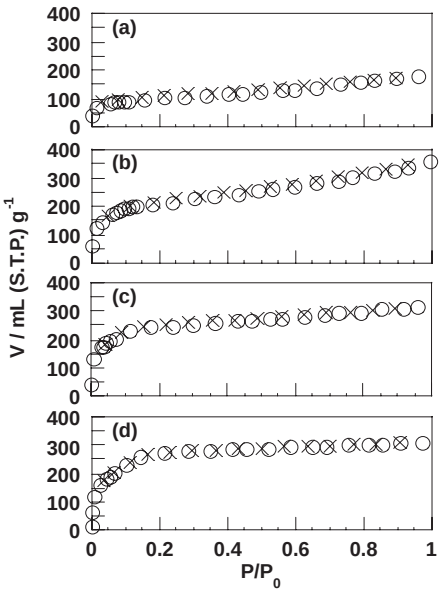

Fig. 8. Nitrogen adsorption/desorption isotherms of (a) CSP (0.67 h), (b) CSP (1 h), (c) CSP (2 h), and (d) CSP (50 h) (adsorption: ○, desorption: ×).

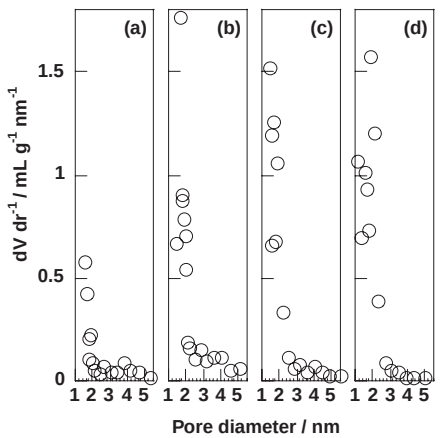

Fig. 9. Pore size distributions derived by the BJH method of (a) CSP (0.67 h), (b) CSP (1 h), (c) CSP (2 h), and (d) CSP (50 h).

during the particle growth (Fig. 5) was one of the possible reasons for the difference of the nanostructures. The BET surface areas were increased (ca. twice) from 0.67 to 1 h, though the CTA^+ content of ASP (1 h) was 1.5 times as large as that of ASP (0.67 h). Accordingly, the rearrangement of the nanostructures during the particle growth was another possibility. The distributions are broad and the pore size is small if compared with those reported for mesoporous silicas prepared by using CTA^+ as supramolecular template such as MCM-41, though the pore sizes of the reported mesoporous silica spherical particles prepared by the Stöber method combined with supramolecular templating approach using CTA^+ are 2–3 nm.[26–35] The inhomegeneous and/or incomplete hydrolysis and the condensation of TEOS as a result of the low synthesis temperature (276 K) in the present study are possible reasons for the nanostructures. Further studies on the pore size and size distribution are required in order to utilize the controlled par-

ticle size practically. The preparation of mesoporous silica spherical particles under different synthetic temperatures and concentrations as well as that using different surfactant templates are underway in our laboratory and the results will be reported subsequently.

Conclusion

Nanoporous silica spherical particles were synthesized by the Stöber method combined with supramolecular templating approach. Tetraethoxysilane and cetyltrimethylammonium chloride were used as silica source and supramolecular template, respectively. The particles which form when the reaction time was shorter than 0.5 h grew while retaining their narrow particle size distribution until the silica source was completely consumed; the particle size reached to ca. 1.8 μm in diameter. Calcination at 823 K led the nanoporous silica spherical particles with the surface areas of 380–1060 $m^2 g^{-1}$ and the pore size of 1.6–2.0 nm.

This work was supported by a Grant-in-Aid for Scientific Research on Priority Areas (417) from the Ministry of Education, Culture, Sports, Science and Technology (MEXT) of the Japanese Government. Waseda University (as a special research project) and Tokuyama Science and Technology Foundation also supported us financially.

References

1 K. Moller and T. Bein, *Chem. Mater.*, **10**, 2950 (1998).
2 A. Stein, B. J. Melde, and R. C. Schroden, *Adv. Mater.*, **12**, 1403 (2000).
3 A. Sayari and S. Hamoudi, *Chem. Mater.*, **13**, 3151 (2001).
4 M. Ogawa, *J. Photochem. Photobiol., C*, **3**, 129 (2002).
5 S. Mann and G. A. Ozin, *Nature*, **382**, 313 (1996).
6 M. Ogawa, *J. Am. Chem. Soc.*, **116**, 7941 (1994).
7 M. Ogawa, *Chem. Commun.*, **1996**, 1149.
8 M. Ogawa and T. Kikuchi, *Adv. Mater.*, **10**, 1077 (1998).
9 R. Ryoo, C. H. Ko, S. J. Cho, and J. M. Kim, *J. Phys. Chem. B*, **101**, 10610 (1997).
10 M. Ogawa, K. Ikeue, and M. Anpo, *Chem. Mater.*, **13**, 2900 (2001).
11 N. Shimura and M. Ogawa, *Bull. Chem. Soc. Jpn.*, **77**, 1599 (2004).
12 M. T. Anderson, J. E. Martin, J. G. Odinek, P. P. Newcomer, and J. P. Wilcoxon, *Microporous Mater.*, **10**, 13 (1997).
13 N. A. Melosh, P. Lipic, F. S. Bates, F. Wudl, G. D. Stucky, G. H. Fredrickson, and B. F. Chmelka, *Macromolecules*, **32**, 4332 (1999).
14 N. A. Melosh, P. Davidson, P. Feng, D. J. Pine, and B. F. Chmelka, *J. Am. Chem. Soc.*, **123**, 1240 (2001).
15 P. J. Bruinsma, A. Y. Kim, J. Liu, and S. Baskaran, *Chem. Mater.*, **9**, 2507 (1997).
16 S. Schacht, Q. Huo, I. G. Voigt-Martin, G. D. Stucky, and F. Schüth, *Science*, **273**, 768 (1996).
17 P. S. Singh and K. Kosuge, *Chem. Lett.*, **1998**, 101.
18 H.-P. Lin, Y.-R. Cheng, and C.-Y. Mou, *Chem. Mater.*, **10**, 3772 (1998).
19 C. E. Fowler, D. Khushalani, and S. Mann, *Chem. Commun.*, **2001**, 2028.
20 H.-P. Lin, C.-Y. Mou, S.-B. Liu, and C.-Y. Tang, *Chem. Commun.*, **2001**, 1970.
21 C. Yu, B. Tian, J. Fan, G. D. Stucky, and D. Zhao, *Chem. Lett.*, **2002**, 62.
22 Q. Sun, P. J. Kooyman, J. G. Grossmann, P. H. H. Bomans, P. M. Frederik, P. C. M. M. Magusin, T. P. M. Beelen, R. A. V. Santen, and N. A. J. M. Sommerdijk, *Adv. Mater.*, **15**, 1097 (2003).
23 M. Ogawa and N. Yamamoto, *Langmuir*, **15**, 2227 (1999).
24 H. M. A. Hunter, A. E. Garcia-Bennett, I. J. Shannon, W. Zhou, and P. A. Wright, *J. Mater. Chem.*, **12**, 20 (2002).
25 G. Zhu, S. Qiu, O. Terasaki, and Y. Wei, *J. Am. Chem. Soc.*, **123**, 7723 (2001).
26 M. Grün, I. Lauer, and K. K. Unger, *Adv. Mater.*, **9**, 254 (1997).
27 K. Schumacher, M. Grün, and K. K. Unger, *Microporous Mesoporous Mater.*, **27**, 201 (1999).
28 M. Grün, K. K. Unger, A. Matsumoto, and K. Tsutsumi, *Microporous Mesoporous Mater.*, **27**, 207 (1999).
29 K. Schumacher, C. D. F. V. Hohenesche, K. K. Unger, R. Ulrich, A. D. Chesne, U. Wiesner, and H. W. Spiess, *Adv. Mater.*, **11**, 1194 (1999).
30 M. Grün, G. Büchel, D. Kumar, K. Schumacher, B. Bidlingmaier, and K. K. Unger, *Stud. Surf. Sci. Catal.*, **128**, 155 (2000).
31 K. Schumacher, S. Renker, K. K. Unger, R. Ulrich, A. D. Chesne, H. W. Spiess, and U. Wiesner, *Stud. Surf. Sci. Catal.*, **129**, 1 (2000).
32 Q. Luo, L. Li, Z. Xue, and D. Zhao, *Stud. Surf. Sci. Catal.*, **129**, 37 (2000).
33 B. Pauwels, G. V. Tendeloo, C. Thoelen, W. V. Rhijn, and P. A. Jacobs, *Adv. Mater.*, **13**, 1317 (2001).
34 R. I. Nooney, D. Thirunavukkarasu, Y. Chen, R. Josephs, and A. E. Ostafin, *Chem. Mater.*, **14**, 4721 (2002).
35 S. Liu, P. Cool, O. Collart, P. V. D. Voort, E. F. Vansant, O. I. Lebedev, G. V. Tendeloo, and M. Jiang, *J. Phys. Chem. B*, **107**, 10405 (2003).
36 K. Yano, N. Suzuki, Y. Akimoto, and Y. Fukushima, *Bull. Chem. Soc. Jpn.*, **75**, 1977 (2002).
37 K. Yano and Y. Fukushima, *J. Mater. Chem.*, **13**, 2577 (2003).
38 K. Yano and Y. Fukushima, *J. Mater. Chem.*, **14**, 1579 (2004).
39 H.-P. Lin and C.-P. Tsai, *Chem. Lett.*, **32**, 1092 (2003).
40 H. Yang, G. Vock, N. Coombs, I. Sokolov, and G. A. Ozin, *J. Mater. Chem.*, **8**, 743 (1998).
41 L. Qi, J. Ma, H. Cheng, and Z. Zhao, *Chem. Mater.*, **10**, 1623 (1998).
42 Q. Cai, Z.-S. Luo, W.-Q. Pang, Y.-W. Fan, X.-H. Chen, and F.-Z. Cui, *Chem. Mater.*, **13**, 258 (2001).
43 Y. Lu, H. Fan, A. Stump, T. L. Ward, T. Rieker, and C. J. Brinker, *Nature*, **398**, 223 (1999).
44 G. V. R. Rao, G. P. López, J. Bravo, H. Pham, A. K. Datye, H. Xu, and T. L. Ward, *Adv. Mater.*, **14**, 1301 (2002).
45 Q. Fu, G. V. R. Rao, L. K. Ista, Y. Wu, B. P. Andrzejewski, L. A. Sklar, T. L. Ward, and G. P. López, *Adv. Mater.*, **15**, 1262 (2003).
46 M. T. Bore, S. B. Rathod, T. L. Ward, and A. K. Datye, *Langmuir*, **19**, 256 (2003).
47 Q. Huo, J. Feng, F. Schüth, and G. D. Stucky, *Chem. Mater.*, **9**, 14 (1997).
48 S. M. Yang, N. Coombs, and G. A. Ozin, *Adv. Mater.*, **12**, 1940 (2000).

49 T. Martin, A. Galarneau, F. D. Renzo, F. Fajula, and D. Plee, *Angew. Chem., Int. Ed.*, **41**, 2590 (2002).

50 T. Martin, A. Galarneau, F. D. Renzo, D. Brunel, F. Fajula, S. Heinisch, G. Crétier, and J.-L. Rocca, *Chem. Mater.*, **16**, 1725 (2004).

51 W. Stöber, A. Fink, and E. Bohn, *J. Colloid Interface Sci.*, **26**, 62 (1968).

52 G. H. Bogush, M. A. Tracy, and C. F. Zukoski, IV, *J. Non-Cryst. Solid.*, **104**, 95 (1988).

53 M. T. J. Keene, R. D. M. Gougeon, R. Denoyel, R. K. Harris, J. Rouquerol, and P. L. Llewellyn, *J. Mater. Chem.*, **9**, 2843 (1999).

54 F. Kleitz, W. Schmidt, and F. Schüth, *Microporous Mesoporous Mater.*, **65**, 1 (2003).

55 S. Brunauer, P. H. Emmett, and E. Teller, *J. Am. Chem. Soc.*, **60**, 309 (1938).

56 E. P. Barrett, L. G. Joyner, and P. P. Halenda, *J. Am. Chem. Soc.*, **73**, 373 (1951).